

NMR Detection of N–H···O=C Hydrogen Bonds in ^{13}C , ^{15}N -Labeled Nucleic Acids

Aizhuo Liu,* Ananya Majumdar, Weidong Hu, Abdelali Kettani, Eugene Skripkin, and Dinshaw J. Patel

Contribution from the Cellular Biochemistry & Biophysics Program, Box 557, Memorial Sloan-Kettering Cancer Center, 1275 York Avenue, New York, New York 10021

Received December 3, 1999

Abstract: We describe the first direct observation of N–H···O=C hydrogen bonding in nucleic acids via the four-bond $^4J_{\text{N}_i\text{N}_j}$ coupling within an $\text{N}_i\text{—H}_i\cdots\text{O}_j\text{=C}_j\text{—N}_j$ segment of a G·G·G·G tetrad. The experiment, two-dimensional (2D) HN(N)-TOCSY, makes use of band-selective ^{15}N isotropic mixing to transfer magnetization exclusively via the $^4J_{\text{NN}}$ couplings to yield correlations between $\text{N}_i\text{H}_i(\omega_2)$ and $\text{N}_j(\omega_1)$ across the hydrogen-bonded segment. In a complementary experiment, 2D cross-polarization (CP)-H(N)CO-(NN)-TOCSY, employing band-selective heteronuclear ^{15}N – ^{13}C cross-polarization sequences on either side of the ^{15}N – ^{15}N TOCSY period, correlations are obtained between $\text{N}_i\text{H}_i(\omega_2)$ and $\text{C}_j(\omega_1)$ nuclei across the hydrogen bond. The symmetric A_2X_2 -type coupling topology of the four-spin nitrogen system in the G·G·G·G tetrad permits accurate measurement of these couplings by a new procedure that fits the experimental data with known analytical isotropic mixing transfer functions. The techniques are demonstrated on a G·G·G·G tetrad formed within a novel dimeric quadruplex fold of a uniformly $^{13}\text{C}/^{15}\text{N}$ -labeled d(G-G-G-T-T-C-A-G-G) DNA sequence. The value of the $^4J_{\text{NN}}$ coupling constant for this system is estimated to be 0.136 ± 0.021 Hz.

Introduction

The recent direct detection of hydrogen bonds by spin–spin scalar couplings between nuclei of hydrogen donor and acceptor moieties in nucleic acids,^{1–5} as well as in proteins,^{6–9} has made possible a new approach for probing hydrogen bonds and provided very important parameters for the characterization of structure and dynamics of biological macromolecules in solution by NMR. These new parameters are particularly valuable for studying nucleic acid polymorphism, where interproton nuclear Overhauser effects (NOEs) are often severely underdetermined. The *trans*- ^{15}N –H··· ^{15}N hydrogen bond scalar couplings ($^2J_{\text{NN}}$) in both RNA and DNA are surprisingly large in the 6–7 Hz range.^{1–3} By contrast, the couplings between the imino hydrogen and its accepting ^{15}N nucleus, $^1J_{\text{HN}}$, are smaller and have values in the 3 Hz range.^{2,3}

The scalar couplings in proteins between the amide nitrogen and carbonyl carbon nucleus, $^3J_{\text{NC}}$, as well as between the

amide proton and carbonyl carbon nucleus, $^2J_{\text{HC}}$, of two residues involved in a N–H···O=C hydrogen bond are of comparable magnitude and generally smaller than 1 Hz.^{6–10} These observations are in agreement with the recent quantum-chemical calculations of the magnitude of scalar couplings between atoms across the hydrogen bond.^{3,11} To date, all attempts to detect ^{15}N –H···O= ^{13}C hydrogen bonds via *trans*-hydrogen bond *J*-couplings ($^3J_{\text{NC}}$) in nucleic acids have failed. This is probably because $^3J_{\text{NC}}$ couplings in nucleic acids are smaller than those in proteins, and also due to the far more complicated nature of *J*-coupling networks in the aromatic rings of nucleic acids relative to those in proteins. In addition, the chemical shift dispersion among aromatic nuclei in base pairs is poor. Direct detection of N–H···O=C hydrogen bonds in nucleic acids represents a challenge that requires the successful design of NMR experiments with both high sensitivity and high selectivity.

In this paper, we report the first direct observation of N–H···O=C hydrogen bonding in nucleic acids via four-bond $^4J_{\text{NN}}$ couplings between nitrogen N_i and N_j linked by $\text{N}_i\text{—H}_i\cdots\text{O}_j\text{=C}_j\text{—N}_j$ hydrogen bonds. Specifically, the coupled ^{15}N nuclei constitute the network of imino (N_i) nitrogens within a G·G·G·G tetrad (Figure 1), found in the d(G-G-G-T-T-C-A-G-G) sequence which adopts a dimeric quadruplex architecture. We present two-dimensional (2D) NMR spectra demonstrating correlations between $\text{N}_i\text{H}_i(\omega_2)$ and $\text{N}_j(\omega_1)$, as well as $\text{N}_i\text{H}_i(\omega_2)$ and $\text{C}_j(\omega_1)$, mediated via $^4J_{\text{NN}}$ couplings between imino (N_i) nitrogens within the G·G·G·G tetrad, in the dimeric d(G-G-G-T-T-C-A-G-G) quadruplex. To detect and quantify these extremely small couplings (~ 0.14 Hz) with high sensitivity, we

* To whom correspondence should be addressed. E-mail: aizhuo@sbnmr1.ski.mskcc.org. Phone: 212-639-7225. Fax: 212-717-3066.

(1) Dingley, A. J.; Grzesiek, S. *J. Am. Chem. Soc.* **1998**, *120*, 8293–8797.

(2) Pervushin, K.; Ono, A.; Fernández, C.; Szyperski, T.; Kainosho, M.; Wüthrich, K. *Proc. Natl. Acad. Sci. U.S.A.* **1998**, *95*, 14147–14151.

(3) Dingley, A. J.; Masse, J. E.; Peterson, R. D.; Barfield, M.; Feigon, J.; Grzesiek, S. *J. Am. Chem. Soc.* **1999**, *121*, 6019–6027.

(4) Majumdar, A.; Kettani, A.; Skripkin, E. *J. Biomol. NMR* **1999**, *14*, 67–70.

(5) Majumdar, A.; Kettani, A.; Skripkin, E.; Patel, D. J. *J. Biomol. NMR* **1999**, *15*, 207–211.

(6) Cordier, F.; Grzesiek, S. *J. Am. Chem. Soc.* **1999**, *121*, 1601–1602.

(7) Cornilescu, G.; Hu, J.-S.; Bax, A. *J. Am. Chem. Soc.* **1999**, *121*, 2949–2950.

(8) Cornilescu, G.; Ramirez, B. E.; Frank, M. K.; Clore, G. M.; Gronenborn, A. M.; Bax, A. *J. Am. Chem. Soc.* **1999**, *121*, 6275–6279.

(9) Wang, Y.-X.; Jacob, J.; Cordier, F.; Wingfield, P.; Stahl, S. J.; Lee-Huang, S.; Torchia, D.; Grzesiek, S.; Bax, A. *J. Biomol. NMR* **1999**, *14*, 181–184.

(10) Cordier, F.; Rogowski, M.; Grzesiek, S.; Bax, A. *J. Magn. Reson.* **1999**, *140*, 510–512.

(11) Scheurer, C.; Brüschweiler, R. *J. Am. Chem. Soc.* **1999**, *121*, 8661–8662.

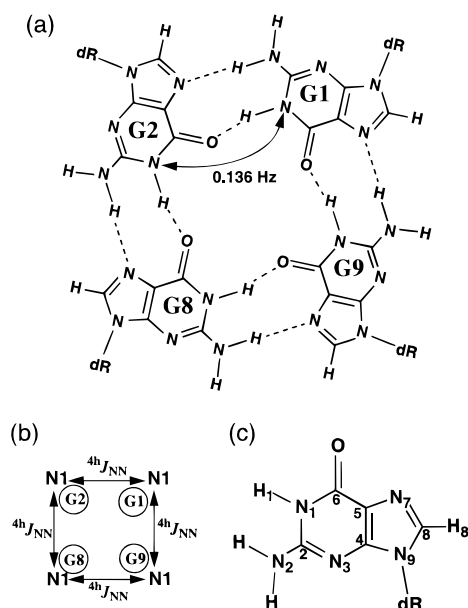


Figure 1. (a) Schematic drawing of one of the two symmetrical G·G·G·G tetrads formed in the dimeric d(G-G-G-T-T-C-A-G-G) quadruplex. Hydrogen bonds are indicated by dashed lines linking the hydrogen and the hydrogen-acceptor atoms. The amplitude of *trans*-hydrogen bond couplings, $^4hJ_{\text{NN}}$, is indicated accordingly with a solid arrow pointing to the corresponding atoms in guanines G1 and G2. (b) The A_2X_2 type J -coupling topology formed by the $^{15}\text{N}1$ spins of four guanines constituting the G·G·G·G tetrad mediated by *trans*-hydrogen bond $^4hJ_{\text{NN}}$ couplings. (c) The chemical structure and numbering of a guanine base according to the IUPAC/IUB nomenclature.^{39,40}

have developed novel NMR techniques employing band-selective ^{15}N - ^{13}C J -cross-polarization. These techniques have been used to establish a new procedure for estimating the $^4hJ_{\text{NN}}$ coupling constants.

The detection of small *trans*-N-H...O=C J -couplings in nucleic acids by NMR requires a procedure for correlating the imino or amino moiety of a base with the carbonyl carbon of its paired partner base, while simultaneously suppressing a similar, and often larger, correlation within the base. The most convenient method to achieve this correlation makes use of insensitive nuclei enhanced polarization transfer (INEPT)¹² steps to transfer magnetization between imino/amino nitrogens and carbonyl carbons. Unfortunately, INEPT-based experiments for detecting small coupling constants within aromatic rings of nucleic acids are often inefficient, due to a number of factors: (i) A large number of homo- and heteronuclear coupling pathways exist, forming a complex network, and are often difficult to isolate from one another. In particular, the $^1J_{\text{NC}}$ couplings of the $^{15}\text{N}1$ nitrogen of guanine to both $^{13}\text{C}6$ (160–163 ppm) and $^{13}\text{C}2$ (152–155 ppm) are similar in magnitude (~ 7.5 Hz).¹³ The proximity of their resonance frequencies renders it almost impossible to isolate the $\text{N}1 \rightarrow \text{C}6$ magnetization-transfer pathway from the $\text{N}1 \rightarrow \text{C}2$ transfer pathway. (ii) During the long delays (~ 200 ms) required for magnetization transfer via small J -couplings, a large number of relaxation processes may come into play, including second-order interactions with remote carbons^{14,15} in the aromatic rings and slow or intermediate conformational exchange effects.¹⁶ The associ-

ated sensitivity losses significantly hamper the determination of extremely small *trans*-hydrogen bond couplings.

A well-known alternative to INEPT-based experiments is J -cross-polarization (CP),¹⁷ which has found several applications in liquid-state NMR primarily as homonuclear (TOCSY,¹⁸ HOHAHA,¹⁹ or isotropic mixing) and, to a more limited extent, as heteronuclear experiments.^{20–22} CP-based experiments possess better radio frequency (rf) inhomogeneity compensation and, in some cases, better relaxation profiles than their INEPT counterparts.^{23,24} CP is often the method of choice for relayed magnetization transfer, especially in the homonuclear case, where the transfer efficiency is far greater than that in INEPT methods.^{17,18} Most applications of CP have been broadband in nature, involving J -coupled spins with wide chemical shift ranges. This necessitates the use of high rf power, especially for hetero-CP experiments involving X-nuclei (e.g., ^{13}C and ^{15}N);²⁴ consequently, the impact of hetero-CP experiments has been somewhat limited. However, for detecting small coupling constants between groups of spins with nearly degenerate chemical shifts, low-power, band-selective CP has significant advantages. With appropriate adjustment of the rf field strength, a high degree of frequency selectivity may be achieved. In this way, magnetization is transferred exclusively between the resonances lying within the applied rf bandwidth, provided that the coupling constants are small, since increased frequency selectivity results in a corresponding increase in the duration of the CP mixing sequence. For magnetization transfer via very small couplings, the increased duration is easily accommodated into the long mixing time required ($\sim 1/2J$ for homo- and $\sim 1/J$ for heteronuclear spin systems) for optimal transfer. A few applications of band-selective CP have been reported in the literature.^{13,25} The pulse sequences described below provide a highly sensitive and frequency-selective procedure for detecting small $^4hJ_{\text{NN}}$ couplings.

Experimental Procedures

NMR experiments were performed on uniformly $^{13}\text{C}/^{15}\text{N}$ -labeled d(G-G-G-T-T-C-A-G-G), which forms a novel dimeric quadruplex containing two G·G·G·G tetrads (Figure 1a). The NMR sample contained a 250- μL volume of 1.0 mM dimeric quadruplex, 100 mM NaCl, and 95% $\text{H}_2\text{O}/5\%$ D_2O at pH 6.5 in a Shigemi microcell. All NMR spectra were collected at 20 $^\circ\text{C}$ on a Varian Inova 600 MHz (^1H) instrument equipped with a z -axis pulsed-field gradient probehead. The time-domain data sets were processed using the program PROSA,²⁶ and the spectra were analyzed using the program XEASY.²⁷

(14) Liu, A.; Riek, R.; Wider, G.; von Schroetter, Ch.; Zahn, R.; Wüthrich, K. *J. Biomol. NMR* **2000**, *16*, 127–138.

(15) Liu, A.; Hu, W.; Qamar, S.; Majumdar, A. *J. Biomol. NMR* **2000**, in press.

(16) Brüschweiler, R.; Ernst, R. R. *J. Chem. Phys.* **1992**, *96*, 1758–1766.

(17) Ernst, R. R.; Bodenhausen, G.; Wokaun, A. *Principles of Nuclear Magnetic Resonance in One and Two Dimensions*; Clarendon Press: Oxford, 1987.

(18) Braunschweiler, L.; Ernst, R. R. *J. Magn. Reson.* **1983**, *53*, 521–528.

(19) Bax, A.; Davis, D. G. *J. Magn. Reson.* **1985**, *65*, 355–360.

(20) Bearden, D. W.; Brown, L. R. *Chem. Phys. Lett.* **1989**, *163*, 432–436.

(21) Zuiderweg, E. R. P. *J. Magn. Reson.* **1990**, *89*, 533–542.

(22) Ernst, M.; Griesinger, C.; Ernst, R. R.; Bermel, W. *Mol. Phys.* **1991**, *74*, 219–252.

(23) Majumdar, A.; Wang, H.; Morshauer, R. C.; Zuiderweg, E. R. P. *J. Biomol. NMR* **1993**, *3*, 387–397.

(24) Majumdar, A.; Zuiderweg, E. R. P. *J. Magn. Reson. Ser. A* **1995**, *113*, 19–31.

(25) Yamazaki, T.; Pascal, S. M.; Singer, A. U.; Forman-Kay, J. D.; Kay, L. E. *J. Am. Chem. Soc.* **1995**, *117*, 3556–3564. Rao, N. S.; Legault, P.; Muhandiram, D. R.; Greenblatt, J.; Battiste, J. L.; Williamson, J. R.; Kay, L. E. *J. Magn. Reson. Ser. B* **1996**, *113*, 272–276.

(12) Morris, G. A.; Freeman, R. *J. Am. Chem. Soc.* **1979**, *101*, 760–762.

(13) Wijmenga, S. S.; van Buuren, B. N. M. *Prog. NMR Spectrosc.* **1998**, *32*, 287–387.

In all NMR experiments, water flip-back pulses²⁸ are applied in appropriate positions to ensure the water magnetization is along the positive *z*-direction during most of the pulse sequence, particularly before acquisition. Residual water is suppressed by WATERGATE²⁹ before detection. The *z*-filtration,^{30,31} preceding or succeeding each CP period, is for selection of in-phase magnetization. For experiments in which the ¹³C6 chemical shift is frequency-labeled during the *t*₁ evolution period, ¹³C5 decoupling is achieved via a ¹³C5-selective 180° pulse in the center of the *t*₁ period.

Results

J-Couplings across hydrogen bonds in a G•G•G•G tetrad (Figure 1) may be manifested via several possible interactions: ^{3h}*J*_{NC'} couplings between ¹⁵N_{*i*} and ¹³C_{6*j*}, as observed in proteins,^{6–9} ^{4h}*J*_{NN} couplings between ¹⁵N_{*i*} and ¹⁵N_{*j*}, and ^{4h}*J*_{CC'} couplings between ¹³C_{6*i*} and ¹³C_{6*j*}. The pulse sequences described below were developed to successfully observe the ^{4h}*J*_{NN} coupling correlation, while attempts were unsuccessful to detect the ^{3h}*J*_{NC'} and ^{4h}*J*_{CC'} coupling correlations.

2D HN(N)-TOCSY Experiment. The pulse sequence for the 2D HN(N)-TOCSY experiment is shown in Figure 2a. The corresponding magnetization-transfer pathway, which is similar to the semi-constant-time (CT) three-dimensional (3D) (H)NNH-TOCSY experiment³² for the measurement of sequential ³*J*_{NN} couplings in proteins, is indicated in the shorthand notation of eq 1. In brief, imino proton magnetization originating from a



guanine base within the G•G•G•G tetrad (Figure 1) is transferred from a guanine nitrogen (N_{*i*}) via an INEPT¹² step, which is then frequency-labeled during the *t*₁ period. After the anti-phase N_{*i*} magnetization is refocused with respect to the imino proton, the N_{*i*} magnetization is subjected to a low-power isotropic mixing with the rf field strength whose bandwidth covers only the N1 chemical shift range (145–148 ppm for guanines, ~200 Hz at 14.1 T). This results in partial magnetization transfer to the N_{*j*} nitrogens of the neighboring guanines in the tetrad via the four-bond ^{4h}*J*_{NN} coupling. An INEPT step then transfers the N_{*i*} magnetization back to its attached proton for detection. The final spectrum correlates the N_{*i*}H_{*j*} proton to the N_{*i*} (auto) and N_{*j*} (cross) nuclei.

A 2D HN(N)-TOCSY spectrum of the dimeric d(G•G•G•T•T•C•A•G•G) quadruplex is shown in Figure 2b, with the corresponding 2D [¹H,¹⁵N]-HSQC reference spectrum shown in Figure 2c. The cross peaks in Figure 2b establish that G1 shows coupling connectivities with G2 and G9, identifying the existence of N1–H•••O=C6 hydrogen bonds between G1•G2 and G1•G9 pairs. Similar hydrogen-bonding interactions are also observed in the G2•G8 pair (Figure 2b). Unfortunately, the imino ¹⁵N1 chemical shifts of G8 and G9 are degenerate, and, therefore, from this spectrum, it is not possible to identify any potential hydrogen bonding in the G8•G9 pair.

(26) Güntert, P.; Dötsch, V.; Wider, G.; Wüthrich, K. *J. Biomol. NMR* **1992**, *2*, 619–629.

(27) Bartels, Ch.; Xia, T.; Billeter, M.; Güntert, P.; Wüthrich, K. *J. Biomol. NMR* **1995**, *6*, 1–10.

(28) Grzesiek, S.; Bax, A. *J. Am. Chem. Soc.* **1993**, *115*, 12593–12594.

(29) Piotto, M.; Saudek, V.; Sklenar, V. *J. Biomol. NMR* **1992**, *2*, 661–665.

(30) Sørensen, O. W.; Rance, M.; Ernst, R. R. *J. Magn. Reson.* **1984**, *56*, 527–534.

(31) Rance, M. *J. Magn. Reson.* **1987**, *74*, 557–564.

(32) Theis, K.; Dingley, A. J.; Hoffmann, A.; Omichinski, J. G.; Grzesiek, S. *J. Biomol. NMR* **1997**, *10*, 403–408.

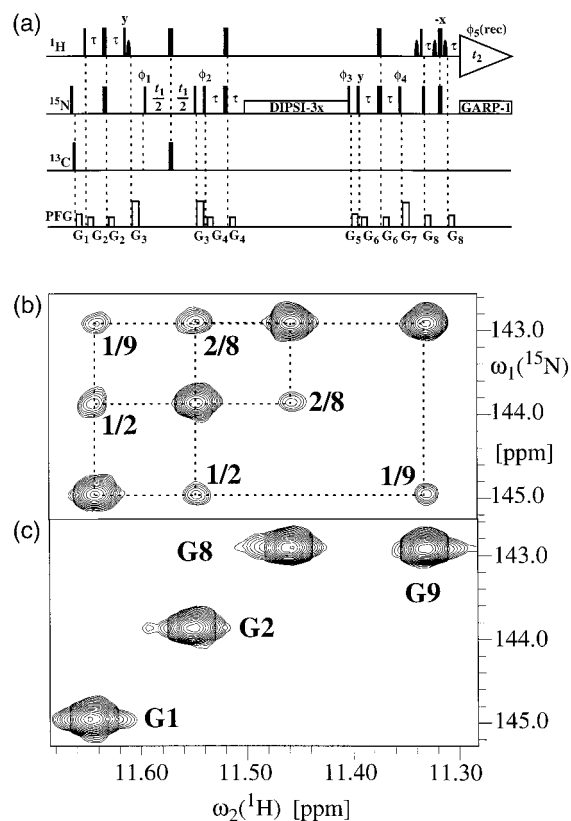


Figure 2. (a) Pulse sequence of the 2D HN(N)-TOCSY experiment that is used for the direct detection of hydrogen bonds by *trans*-hydrogen bond ^{4h}*J*_{NN} couplings within the G•G•G•G tetrads in the dimeric quadruplex. The ^{4h}*J*_{NN} couplings are active during the imino nitrogen isotropic mixing period. Narrow and wide rectangular black bars indicate nonselective 90° and 180° pulses, respectively. Unless indicated otherwise, the pulses are applied with phase *x*. The ¹H, ¹⁵N, and ¹³C carrier frequencies are set at 4.78 (water), 143.94 (guanine imino ¹⁵N₁), and 162.09 ppm (guanine carbonyl ¹³C₆), respectively. The nonselective proton pulses are applied using a 37.9 kHz field strength. The selective ¹H 90° pulses, indicated with black bell-shaped bars, used for water flip-back²⁸ are rectangular pulses of duration 1.7 ms. The ¹⁵N pulses are applied with a field strength of 6.1 kHz, and ¹⁵N decoupling using the GARP-1 sequence⁴¹ with 1.0 kHz is applied during acquisition. The field strengths of (DIPSI-3)*x* or (DIPSI-2)*x*^{35,36} used for the imino ¹⁵N₁ isotropic mixing are set to 286.8 (90° pulse of 871.8 μs) and 361 Hz (90° pulse of 692.5 μs), respectively. The delay *τ* employed is 2.65 ms. The phase cycling scheme used is $\phi_1 = x, -x; \phi_2 = 2(x), 2(-x); \phi_3 = 4(y), 4(-y); \phi_4 = 8(x), 8(-x); \phi_5(\text{rec}) = A, B, B, A$, where $A = x, -x, -x, x$ and $B = A + 180^\circ$. Quadrature detection in the $\omega_1(^{15}\text{N})$ dimension is achieved using States-time-proportional phase incrementation (TPPI)⁴² phase cycling of ϕ_1 . The durations and strengths of the *z*-axis pulsed field gradients employed are as follow: $G_1 = 1.5$ ms, 20 G/cm; $G_2 = 0.5$ ms, 7 G/cm; $G_3 = 1.0$ ms, 25 G/cm; $G_4 = 0.5$ ms, 6 G/cm; $G_5 = 0.8$ ms, 15 G/cm; $G_6 = 0.5$ ms, 8 G/cm; $G_7 = 1.0$ ms, 20 G/cm; and $G_8 = 0.4$ ms, 18 G/cm. (b) 2D HN(N)-TOCSY spectrum collected with the pulse sequence of (a). (c) 2D [¹H,¹⁵N]-HSQC reference spectrum associated with the G•G•G•G tetrad in the dimeric quadruplex. Both spectra b and c were recorded with acquisition times of $t_{1\text{max}}(^{15}\text{N}) = 120$ ms and $t_{2\text{max}}(^1\text{H}) = 93$ ms in the two dimensions, respectively. The imino nitrogen isotropic mixing time for the 2D HN(N)-TOCSY spectrum was set to 379 ms with the (DIPSI-3)*x* sequence^{35,36} and 96 scans per *t*₁ increment. The total experimental time was about 2 h. The auto imino resonances of the guanine tetrad have been assigned to the individual bases and are indicated in panel c. The cross peaks of *trans*-hydrogen bond correlation signals are indicated accordingly in panel b.

2D CP-H(N)CO-(NN)-TOCSY Experiment. Complementary to the 2D HN(N)-TOCSY experiment is the 2D CP-H(N)-

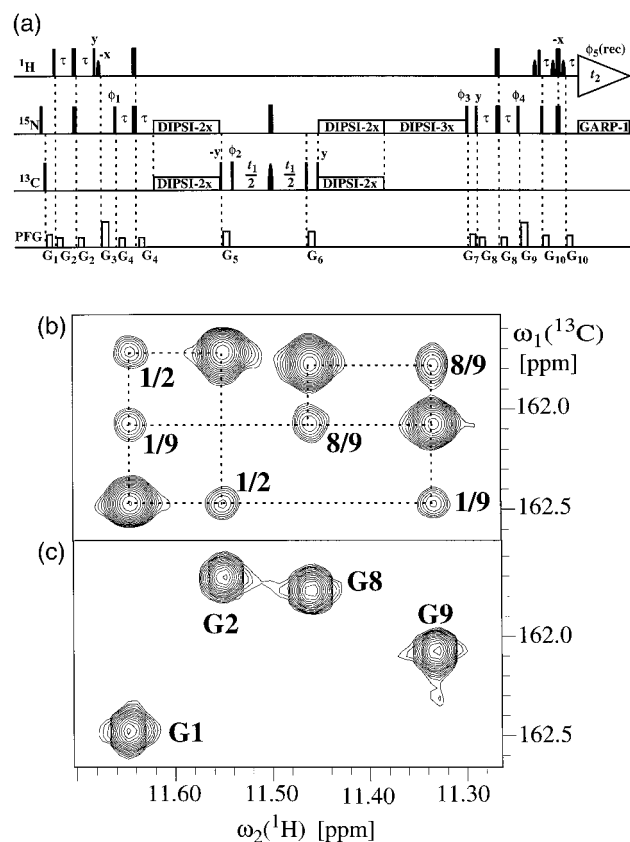


Figure 3. (a) Pulse sequence of 2D CP-H(N)CO-(NN)-TOCSY experiment which is complementary to the experiment of 2D HN(N)-TOCSY shown in Figure 2a. The field strengths (361 Hz, 90° pulse of 692.5 μs using (DIPSI-2)x^{35,36}) and lengths of the two imino nitrogen/carbonyl carbon cross-polarization periods that flank the *t*₁ carbonyl carbon chemical shift evolution period were adjusted to optimize the magnetization transfer within a guanine base via the one-bond ¹J_{NC'} coupling. The ¹³C5 180° selective decoupling pulse in the middle of *t*₁ evolution period is applied as a 130-μs cosine-modulated rectangular pulse centered at 118 ppm, and an off-resonance compensation pulse is applied at the end of the *t*₁ period. Other parameters and the phase cycling scheme used are the same as those in Figure 2a. Quadrature detection in the ω₁(¹³C) dimension is achieved with States-TPPI⁴² by increasing the phase φ₂. The durations and strengths of the z-axis pulsed field gradients used are as follow: G₃ = 1.0 ms, 25 G/cm; G₄ = 0.5 ms, 6 G/cm; G₅ = 0.8 ms, 14 G/cm; G₆ = 0.8 ms, 12 G/cm; G₇ = 0.8 ms, 15 G/cm; G₈ = 0.5 ms, 8 G/cm; G₉ = 1.0 ms, 20 G/cm; and G₁₀ = 0.4 ms, 18 G/cm. (b) 2D CP-H(N)CO-(NN)-TOCSY spectrum recorded using the pulse sequence of (a). (c) 2D H(N)CO reference spectrum associated with the G•G•G•G tetrad in the dimeric quadruplex. Both spectra b and c were recorded with acquisition times of *t*_{1max}(¹³C) = 80 ms and *t*_{2max}(¹H) = 93 ms in the two dimensions, respectively. The imino nitrogen/carbonyl carbon cross-polarization period was set to 80 ms, which is a compromise between maximal magnetization transfer within a guanine base via the one-bond ¹J_{NC'} coupling and minimal relaxation and interference of long-range couplings. The imino nitrogen isotropic mixing time was set to 379 ms with (DIPSI-3)x sequence^{35,36} and 256 scans per *t*₁ increment, which resulted in 4.8 h of experimental time. The carbonyl carbon resonances of the guanine tetrad have been assigned to the individual bases and are indicated in panel c, and the *trans*-hydrogen bond correlation signals are indicated accordingly in panel b.

CO-(NN)-TOCSY experiment. The pulse sequence (Figure 3a) is outlined below:

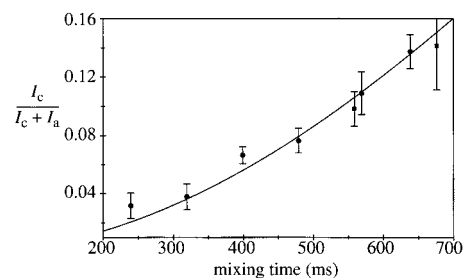
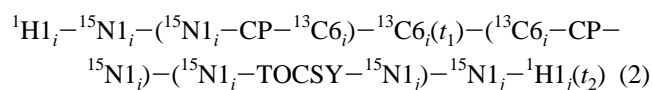


Figure 4. Best fit of normalized intensities, $I_c/(I_c + I_a) = R(\tau_m)/[1 + R(\tau_m)]$, of *trans*-hydrogen bond correlation peaks in the 2D HN(N)-TOCSY spectra with analytical expressions (see eqs 3 and 4) for polarization transfer efficiency in the four-spin A₂X₂-type system represented by the imino nitrogens of G•G•G•G tetrads (Figure 1) under isotropic mixing conditions. *I*_c and *I*_a are intensities of cross peaks and auto peaks, respectively, and $R(\tau_m) = T_c/T_a$ is the ratio of polarization transfer efficiencies of (*T*_c) cross peaks and (*T*_a) auto peaks. Eight spectra were collected with isotropic mixing times $\tau_m = 239.36, 319.15, 398.93, 478.72, 558.51, 568.85, 638.29, \text{ and } 676.05$ ms using either DIPSI-2 (●) or DIPSI-3 (■) sequences.^{35,36} The estimated average value of the *trans*-hydrogen bond *J*-couplings is ${}^4\text{h}J_{\text{NN}} = 0.136 \pm 0.021$ Hz. Error bars correspond to propagated errors derived from the noise of the spectra. Auto peaks of G8 and G9 (see Figure 3) were not included in the calculation due to their degenerate ¹⁵N1 chemical shifts. Cross peaks linking G1 and G9 were also excluded to minimize the propagated errors stemming from carrier offset effects.

Briefly, a refocused H → N INEPT transfer process generates in-phase N1_{*i*} magnetization, which is transferred to the intrarésidue C6_{*i*} carbon via band-selective hetero-(¹⁵N,¹³C)-cross-polarization. The C6_{*i*} carbon is frequency-labeled during *t*₁ and then transferred back to N1_{*i*} via a reverse (¹⁵N,¹³C)-CP step. A subsequent band-selective ¹⁵N-¹⁵N isotropic mixing step, as in the 2D HN(N)-TOCSY sequence, partially transfers N1_{*i*} magnetization to N1_{*j*} via the ⁴hJ_{NN} coupling, which is detected via an INEPT step, on the N1H_{*j*} proton. The final spectrum correlates N1H_{*j*} (ω₂) with C6_{*j*} (auto) and C6_{*i*} (cross).

The 2D CP-H(N)CO-(NN)-TOCSY spectrum of the dimeric d(G•G•G•T•T•C•A•G•G) quadruplex is shown in Figure 3b. The corresponding 2D H(N)CO reference spectrum is shown in Figure 3c. The ¹³C6 resonances of G8 and G9 are nondegenerate, and, therefore, the presence of N-H...O=C hydrogen bonds across the G8•G9 pair is easily established from the N1H(G9)-C6(G8) cross peaks. The observation of NH(G1)-C6(G2) and N1H(G1)-C6(G9) cross peaks confirms the G1•G2 and G1•G9 pairings as established from the HN(N)-TOCSY experiment. In contrast, the ¹³C6 chemical shifts of G2 and G8 are degenerate, thereby precluding the establishment of the G2•G8 base pairing, which is readily observable in the HN(N)-TOCSY spectrum. In combination, Figures 3 and 4 not only serve to clearly demonstrate the presence of ⁴hJ_{NN} couplings but also emphasize the complementarity of the HN(N)-TOCSY and H(N)CO-(NN)-TOCSY experiments.

Other CP-Based NMR Experiments. The same principles have been used to construct the 2D CP-HN(CO) (see Figure S1a, Supporting Information) and 2D CP-H(N)CO (Figure S1b, Supporting Information) experiments which transfer magnetization via potential ³hJ_{NC'} couplings, and the 2D CP-H(N)CO-(CC)-TOCSY (Figure S1c, Supporting Information) experiment which makes use of ⁴hJ_{CC'} couplings. These pulse sequences are described in the Supporting Information. Despite our best efforts we were unable to detect the ³hJ_{NC'} and ⁴hJ_{CC'} coupling correlations as outlined in the Discussion section.

⁴hJ_{NN} Couplings. Luy et al.³³ have devised general analytical expressions of polarization transfer functions for a scalar-coupled

four-spin- $1/2$ system under isotropic mixing conditions in the absence of relaxation. For the G•G•G•G tetrad (Figure 1a), each of the four imino $^{15}\text{N}_1$ spins is coupled with its two neighbors via four-bond *trans*-hydrogen bond couplings, $^4J_{\text{NN}}$, constituting a symmetric A_2X_2 type of coupling topology (Figure 1b). The transfer functions for cross peak (T_c) and auto peak (T_a) intensities are given by the following equations, which are valid for isotropic mixing in an A_2X_2 spin system:^{33,34}

$$T_c = 1/6 \{1 - \cos(2\pi J\tau_m)\} + 5/24 \{1 - \cos(4\pi J\tau_m)\} \quad (3)$$

$$T_a = 1 - 1/6 \{1 - \cos(2\pi J\tau_m)\} - 5/24 \{1 - \cos(4\pi J\tau_m)\} = 1 - T_c \quad (4)$$

where J represents the *trans*-hydrogen bond couplings ($^4J_{\text{NN}}$) linking the imino $^{15}\text{N}_1$ spins of adjacent guanine bases and τ_m is the $^{15}\text{N}_1$ isotropic mixing time. Thus, assuming identical relaxation rates for auto and cross peaks, and knowing the intensity ratio, $R(\tau_m) = T_c/T_a$, obtained from a series of 2D spectra with different mixing times, the value of J can be obtained by fitting the experimental data with the analytical curve: $R(\tau_m)/[1 + R(\tau_m)] = T_c$.

A series of 2D HN(N)-TOCSY spectra were collected using (DIPSI-2)x and (DIPSI-3)x^{35,36} sequences with 8 different mixing times (τ_m) in order to obtain a quantitative estimate of $^4J_{\text{NN}}$ couplings. The best fit of the experimental data with the analytical curve of $R(\tau_m)/[1 + R(\tau_m)]$ (see above) using eqs 3 and 4 is plotted in Figure 4. The value of the $^4J_{\text{NN}}$ coupling was determined to be 0.136 ± 0.021 Hz.

Discussion

In this study, our primary objective has been to detect N—H•••O=C hydrogen bonds in nucleic acids. Following the strategies adopted in proteins, the natural choice in this direction was to attempt observation of $^3J_{\text{NC}'\text{C}'}$ couplings, for which we targeted the N1—H•••O=C6—N1 hydrogen bonds of a stable G•G•G•G tetrad (Figure 1a) within a ^{13}C , ^{15}N -labeled dimeric d(G-G-G-T-T-C-A-G-G) quadruplex. After repeated lack of success using INEPT-based HNC0-type experiments, we switched to band-selective cross-polarization using the 2D CP-HN(CO) (see Figure S1a, Supporting Information) and 2D CP-H(N)CO (see Figure S1b, Supporting Information) experiments, in attempts to obtain N1—H_{*i*}—O=C_{*6j*} correlations. Indeed, the CP-H(N)CO experiment turned out to be far more sensitive than the corresponding CT-H(N)CO³⁷ experiment in this case. Disappointingly, however, no *trans*-hydrogen bond N1_{*i*}—H•••O=C_{*6j*} correlations could be detected. At this point, the carbon carrier frequency was mistakenly positioned at 13 ppm upfield of the $^{13}\text{C}_6$ nuclei in the 2D CP-HN(CO) experiment. To our surprise, the experiment turned out to be so sensitive that all the expected N1—H_{*i*}—O=C_{*6j*}—N_{*j*} cross peaks could be observed within 1 h of data collection (Figure 2b). The spectrum remained unaffected even after complete elimination of any CP

mixing on ^{13}C ! In essence, the accidental offset mismatching of the ^{13}C carrier had transformed the CP—HN(CO) experiment into an HN(N)-TOCSY experiment (Figure 2a), resulting in band-selective magnetization transfer exclusively via the $^4J_{\text{NN}}$ coupling between $^{15}\text{N}_1$ nuclei. This also explains why $^3J_{\text{NC}'\text{C}'}$ couplings could not be observed directly. In the CP-H(N)CO and CP-HN(CO) experiments, during the ^{15}N — ^{13}C CP mixing period, adjusted for refocusing of the $^1J_{\text{NC}'\text{C}'}$ coupling, transfer via the $^3J_{\text{NC}'\text{C}'}$ coupling competes unfavorably with the far more efficient homonuclear ^{15}N — ^{15}N TOCSY transfer, which is active simultaneously. This is likely to be true even if the $^3J_{\text{NC}'\text{C}'}$ coupling is twice as large as the $^4J_{\text{NN}}$ coupling observed in the work. In principle, the $^4J_{\text{C}'\text{C}'}$ coupling can provide an additional competitive pathway. However, in this work, no evidence for $^4J_{\text{C}'\text{C}'}$ couplings could be observed using the CP-H(N)CO—(CC)-TOCSY experiment (see Figure S1c, Supporting Information). The lack of cross peaks in the $^3J_{\text{NC}'\text{C}'}$ correlation experiments is, therefore, likely due to the interference of the $^4J_{\text{NN}}$ alone.

The unique spin-coupling topology of the G•G•G•G tetrad allows quantification of the $^4J_{\text{NN}}$ couplings with not only high sensitivity but also high accuracy. The magnitudes of the observed four-bond $^4J_{\text{NN}}$ coupling (~ 0.14 Hz) in nucleic acids can be compared with the three-bond $^3J_{\text{NC}'\text{C}'}$ coupling (~ 0.5 Hz) in proteins^{6–9} and the two-bond $^2J_{\text{NN}}$ coupling (6–7 Hz) in nucleic acids.^{1–3} The detection of the $^4J_{\text{NN}}$ coupling but not the $^4J_{\text{C}'\text{C}'}$ coupling probably reflects the larger electronegativity of the nitrogen atom in comparison with the carbon atom. Interestingly, the magnitudes of $^4J_{\text{NN}}$ couplings reported here are in the same range as the sequential $^3J_{\text{NN}}$ couplings measured in proteins.³² Whether the *trans*-hydrogen bond $^4J_{\text{NN}}$ couplings in proteins are measurable or negligibly small remains unestablished at this time. Most importantly, the N—H•••O=C hydrogen bonds are as ubiquitous as the N—H•••N hydrogen bonds in nucleic acids, as well as in protein/nucleic acid complexes, and they play a key role in nucleic acid architecture stabilization and molecular recognition.³⁸ The first direct detection of the N—H•••O=C hydrogen bonds in nucleic acids by *trans*-hydrogen bond J -couplings, together with the known observation of N—H•••N hydrogen bonds via the much larger couplings,^{1–3} should provide critical restraints in nucleic acid solution structure determination and in the characterization of intermolecular interactions.

Acknowledgment. This research was supported by NIH Grant GM34504 to D.J.P..

Supporting Information Available: One figure showing the pulse sequences of 2D CP-HN(CO), 2D CP-H(N)CO, and 2D CP-H(N)CO—(CC)-TOCSY experiments and associated text (PDF). This material is available free of charge via the Internet at <http://pubs.acs.org>.

JA994255S

(38) Jeffrey, G. A.; Saenger, W. *Hydrogen Bonding in Biological Structures*; Springer, Berlin, 1991.

(39) IUPAC—IUB Joint Commission on Biochemical Nomenclature. *Eur. J. Biochem.* **1983**, *131*, 9–15.

(40) Markley, J. L.; Bax, A.; Arata, Y.; Hilbers, C. W.; Kaptein, R.; Skyes, B. D.; Wright, P. E.; Wüthrich, K. *J. Biomol. NMR* **1998**, *12*, 1–23.

(41) Shaka, A. J.; Barker, P. B.; Freeman, R. J. *Magn. Reson.* **1985**, *64*, 547–552.

(42) Marion, D.; Ikura, M.; Tschudin, R.; Bax, A. *J. Magn. Reson.* **1989**, *85*, 393–399.

(33) Luy, B.; Schedletzy, O.; Glaser, S. J. *J. Magn. Reson.* **1999**, *138*, 19–27.

(34) Chandrakumar, N.; Visalakshi, G. V.; Ramaswamy, D.; Subramanian, S. *J. Magn. Reson.* **1986**, *67*, 307–318.

(35) Shaka, A. J.; Lee, C. J.; Pines, A. *J. Magn. Reson.* **1988**, *77*, 274–293.

(36) Cavanagh, J.; Rance, M. *J. Magn. Reson.* **1992**, *96*, 670–678.

(37) Grzesiek, S.; Bax, A. *J. Magn. Reson.* **1992**, *96*, 432–440.